Research Article | Vol. 24, No. 25 | 12 Dec 2016 | OPTICS EXPRESS 29033

Optics EXPRESS

White-light diffraction phase microscopy at doubled space-bandwidth product

MINGGUANG SHAN,[1,2] MIKHAIL E. KANDEL,[1] HASSAAN MAJEED,[1] VIOREL NASTASA,[1,3] AND GABRIEL POPESCU[1,*]

[1]*Quantitative Light Imaging Laboratory, Department of Electrical and Computer Engineering, Beckman Institute for Advanced Science and Technology, University of Illinois at Urbana-Champaign, Urbana, Illinois 61801, USA*
[2]*College of Information and Communication Engineering, Harbin Engineering University, Harbin, Heilongjiang 150001, China*
[3]*National Institute for Laser Plasma and Radiation Physics, Magurele, Ilfov 077125, Romania*
**gpopescu@illinois.edu*

Abstract: White light diffraction microscopy (wDPM) is a quantitative phase imaging method that benefits from both temporal and spatial phase sensitivity, granted, respectively, by the common-path geometry and white light illumination. However, like all off-axis quantitative phase imaging methods, wDPM is characterized by a reduced space-bandwidth product compared to phase shifting approaches. This happens essentially because the ultimate resolution of the image is governed by the period of the interferogram and not just the diffraction limit. As a result, off-axis techniques generates single-shot, i.e., high time-bandwidth, phase measurements, at the expense of either spatial resolution or field of view. Here, we show that combining phase-shifting and off-axis, the original space-bandwidth is preserved. Specifically, we developed phase-shifting diffraction phase microscopy with white light, in which we measure and combine two phase shifted interferograms. Due to the white light illumination, the phase images are characterized by low spatial noise, i.e., <1nm pathlength. We illustrate the operation of the instrument with test samples, blood cells, and unlabeled prostate tissue biopsy.

OCIS codes: (180.3170) Interference microscopy; (170.0110) Imaging systems; (120.5050) Phase measurement; (999.9999) Quantitative phase imaging.

References and links

1. G. Popescu, *Quantitative Phase Imaging of Cells and Tissues* (McGraw-Hill, 2011).
2. L. Miccio, A. Finizio, R. Puglisi, D. Balduzzi, A. Galli, and P. Ferraro, "Dynamic DIC by digital holography microscopy for enhancing phase-contrast visualization," Biomed. Opt. Express **2**(2), 331–344 (2011).
3. B. Rappaz, P. Marquet, E. Cuche, Y. Emery, C. Depeursinge, and P. Magistretti, "Measurement of the integral refractive index and dynamic cell morphometry of living cells with digital holographic microscopy," Opt. Express **13**(23), 9361–9373 (2005).
4. B. Kemper, A. Bauwens, A. Vollmer, S. Ketelhut, P. Langehanenberg, J. Müthing, H. Karch, and G. von Bally, "Label-free quantitative cell division monitoring of endothelial cells by digital holographic microscopy," J. Biomed. Opt. **15**(3), 036009 (2010).
5. N. T. Shaked, T. M. Newpher, M. D. Ehlers, and A. Wax, "Parallel on-axis holographic phase microscopy of biological cells and unicellular microorganism dynamics," Appl. Opt. **49**(15), 2872–2878 (2010).
6. P. Bon, S. Aknoun, S. Monneret, and B. Wattellier, "Enhanced 3D spatial resolution in quantitative phase microscopy using spatially incoherent illumination," Opt. Express **22**(7), 8654–8671 (2014).
7. N. Warnasooriya and M. K. Kim, "LED-based multi-wavelength phase imaging interference microscopy," Opt. Express **15**(15), 9239–9247 (2007).
8. P. Kolman and R. Chmelík, "Coherence-controlled holographic microscope," Opt. Express **18**(21), 21990–22003 (2010).
9. V. P. Pandiyan and R. John, "Optofluidic bioimaging platform for quantitative phase imaging of lab on a chip devices using digital holographic microscopy," Appl. Opt. **55**(3), A54–A59 (2016).
10. Y. Park, C. A. Best, K. Badizadegan, R. R. Dasari, M. S. Feld, T. Kuriabova, M. L. Henle, A. J. Levine, and G. Popescu, "Measurement of red blood cell mechanics during morphological changes," Proc. Natl. Acad. Sci. U.S.A. **107**(15), 6731–6736 (2010).

#278338 http://dx.doi.org/10.1364/OE.24.029039
Journal © 2016 Received 7 Oct 2016; revised 28 Oct 2016; accepted 1 Nov 2016; published 7 Dec 2016

Optics EXPRESS

11. H. V. Pham, B. Bhaduri, K. Tangella, C. Best-Popescu, and G. Popescu, "Real time blood testing using quantitative phase imaging," PLoS One **8**(2), e55676 (2013).
12. M. Mir, Z. Wang, K. Tangella, and G. Popescu, "Diffraction Phase Cytometry: blood on a CD-ROM," Opt. Express **17**(4), 2579–2585 (2009).
13. Y. Park, C. A. Best-Popescu, R. R. Dasari, and G. Popescu, "Light scattering of human red blood cells during metabolic remodeling of the membrane," J. Biomed. Opt. **16**(1), 011013 (2011).
14. Y. Park, M. Diez-Silva, G. Popescu, G. Lykotrafitis, W. Choi, M. S. Feld, and S. Suresh, "Refractive index maps and membrane dynamics of human red blood cells parasitized by Plasmodium falciparum," Proc. Natl. Acad. Sci. U.S.A. **105**(37), 13730–13735 (2008).
15. M. Mir, A. Bergamaschi, B. S. Katzenellenbogen, and G. Popescu, "Highly sensitive quantitative imaging for monitoring single cancer cell growth kinetics and drug response," PLoS One **9**(2), e89000 (2014).
16. G. Popescu, Y. Park, N. Lue, C. Best-Popescu, L. Deflores, R. R. Dasari, M. S. Feld, and K. Badizadegan, "Optical imaging of cell mass and growth dynamics," Am. J. Physiol. Cell Physiol. **295**(2), C538–C544 (2008).
17. S. Ceballos, M. Kandel, S. Sridharan, H. Majeed, F. Monroy, and G. Popescu, "Active intracellular transport in metastatic cells studied by spatial light interference microscopy," J. Biomed. Opt. **20**(11), 111209 (2015).
18. M. Mir, T. Kim, A. Majumder, M. Xiang, R. Wang, S. C. Liu, M. U. Gillette, S. Stice, and G. Popescu, "Corrigendum: Label-Free Characterization of Emerging Human Neuronal Networks," Sci. Rep. **5**, 11311 (2015).
19. R. Wang, Z. Wang, L. Millet, M. U. Gillette, A. J. Levine, and G. Popescu, "Dispersion-relation phase spectroscopy of intracellular transport," Opt. Express **19**(21), 20571–20579 (2011).
20. S. Sridharan, V. Macias, K. Tangella, A. Kajdacsy-Balla, and G. Popescu, "Prediction of prostate cancer recurrence using quantitative phase imaging," Sci. Rep. **5**, 9976 (2015).
21. Z. Wang, K. Tangella, A. Balla, and G. Popescu, "Tissue refractive index as marker of disease," J. Biomed. Opt. **16**(11), 116017 (2011).
22. S. Uttam, H. V. Pham, J. LaFace, B. Leibowitz, J. Yu, R. E. Brand, D. J. Hartman, and Y. Liu, "Early prediction of cancer progression by depth-resolved nanoscale mapping of nuclear architecture from unstained tissue specimens," Cancer Res. **75**(22), 4718–4727 (2015).
23. D. Paganin and K. A. Nugent, "Noninterferometric phase imaging with partially coherent light," Phys. Rev. Lett. **80**(12), 2586–2589 (1998).
24. N. T. Shaked, Y. Zhu, M. T. Rinehart, and A. Wax, "Two-step-only phase-shifting interferometry with optimized detector bandwidth for microscopy of live cells," Opt. Express **17**(18), 15585–15591 (2009).
25. C. Edwards, B. Bhaduri, B. G. Griffin, L. L. Goddard, and G. Popescu, "Epi-illumination diffraction phase microscopy with white light," Opt. Lett. **39**(21), 6162–6165 (2014).
26. B. Bhaduri, C. Edwards, H. Pham, R. Zhou, T. H. Nguyen, L. L. Goddard, and G. Popescu, "Diffraction phase microscopy: principles and applications in materials and life sciences," Adv. Opt. Photonics **6**(1), 57–119 (2014).
27. H. Pham, B. Bhaduri, H. Ding, and G. Popescu, "Spectroscopic diffraction phase microscopy," Opt. Lett. **37**(16), 3438–3440 (2012).
28. B. Bhaduri, H. Pham, M. Mir, and G. Popescu, "Diffraction phase microscopy with white light," Opt. Lett. **37**(6), 1094–1096 (2012).
29. G. Popescu, T. Ikeda, R. R. Dasari, and M. S. Feld, "Diffraction phase microscopy for quantifying cell structure and dynamics," Opt. Lett. **31**(6), 775–777 (2006).

1. Introduction

Quantitative phase imaging (QPI) has been receiving intense scientific interest as a new modality for label-free biomedical optical imaging [1]. QPI can investigate unlabeled specimens, by converting optical pathlength data into biologically-relevant information [2–10]. Since the optical phase delay introduced by the specimen depends on both its thickness and refractive index, which essentially represents density, QPI has been used in a variety of applications, including topography and volume try of red blood cells [11, 12], cell membrane fluctuations [13, 14], cell growth [15, 16], intracellular mass transport [17–19], cancer diagnosis in biopsies [20–22].

In terms of instrumentation, all QPI approaches rely on interference, because experimentally we only have access to phase differences between two fields, or, equivalently, the phase of cross-correlation functions and not of the fields themselves. Sometimes, in-line holographic setups, e.g., transport of intensity methods are termed "non-interferometric" [23], likely because they do not involve a classical interferometer, in which two beams are physically separated. However, even in this case the phase information is experimentally extracted from the interferogram generated by the incident and scatter light. In order to decouple the phase and amplitude information, several intensity measurements are developed

Optics EXPRESS

at different phase shifts between the two fields. This class of instruments is referred to as *phase-shifting*.

The second type of QPI instruments is called *off-axis*. Unlike phase-shifting methods, the off-axis ones provide single-shot phase information, thus allowing for much faster acquisition rates. However, this high *time-bandwidth* method comes at the expense of the *space-bandwidth* product, i.e., in off-axis geometries one has to compromise either spatial resolution or field of view. Slightly off-axis geometries [24] combining off-axis and phase-shifting can provide a trade-off between the time-bandwidth product and space-bandwidth product for accurate QPI instruments.

In this paper we present a new QPI method, referred to as phase shifting diffraction phase microscopy with white light (PSwDPM), which can retrieve the unaltered space-bandwidth product in diffraction phase microscopy (DPM) [25–29]. In terms of the advancement with respect to Ref. 24, we would like to point out that our method provides two key improvements. 1) the geometry is common path and, as a result, the temporal stability is intrinsically better than in traditional Mach-Zehnder interferometers. 2) The white light illumination provides speckle-free images, which otherwise plague the laser methods. Due to these two improvements, our measurements are both temporally and spatially more sensitive.

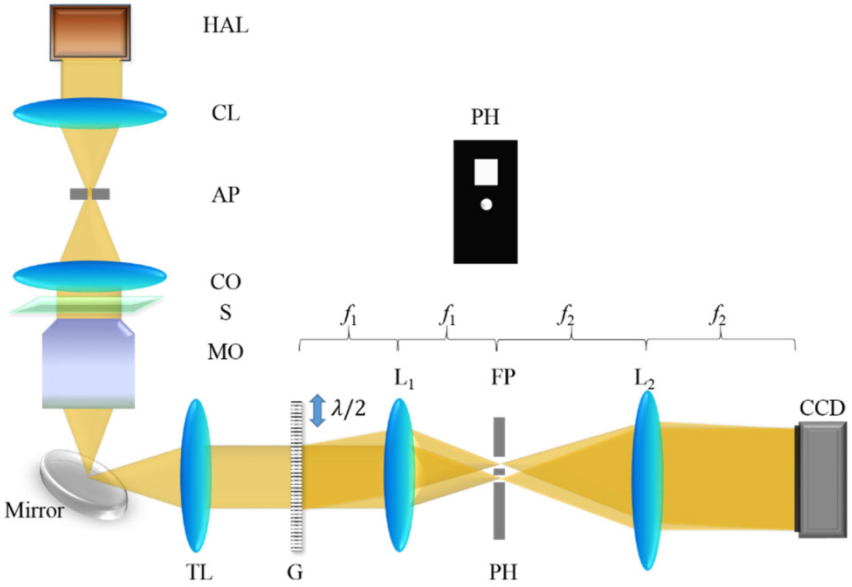

Fig. 1. PSwDPM setup. Abbreviations: HAL, Halogen Lamp; CL, Collector Lens; AP, Aperture; CO, Condenser; S, Sample; MO, Microscope Objective; TL, Tube Lens; G, Grating; L1/L2, Lens; PH, Pinhole; FP, Fourier Plane.

2. Theory

The PSwDPM setup is shown in Fig. 1. An inverted microscope is equipped with a halogen lamp, whose light is spatially filtered by a condenser aperture. Thus, the sample is illuminated by a collimated white light beam. The microscope generates a diffraction-limited image at its output port. Precisely at the image plane, we place a diffraction grating, of 33.33 lines/mm. The grating generates diffraction orders, out of which we use two: the 0th and 1st order. Essentially, the grating is used to form a compact Mach–Zehnder type interferometer. In order to covert the 0th order into the reference field of the interferometer, we spatially filter it using Lens L1 and a pinhole. Lens L2 is forming back the image at the CCD plane. The interferogram recorded by the CCD consists of the original image, carried by the 1st order of diffraction, overlapped with the off-axis reference, given by the 0th order. Because of the

Optics EXPRESS

common-path geometry, DPM is extremely stable, resulting in temporal pathlength noise of <1nm, without active stabilization measurers [26]. The measured irradiance distribution has the form

$$I(x,y) = I_0 + I_1 + 2\sqrt{I_0 I_1}\cos\left[\phi(x,y) + \alpha x\right] \tag{1}$$

where I_0 and I_1 are the irradiance of the 0th and 1st order, respectively, and ϕ is the phase map of interest. The spatial frequency, $\alpha = 2\pi/\Lambda$, is due to the grating, with Λ is the period of the grating. In order to establish the sampling conditions for the interferogram, we perform a spatial frequency domain analysis. Taking the Fourier transform of the measured intensity, we obtain

$$\begin{aligned}\tilde{I}(k_x,k_y) = \Im[&U_0 U_0^* + U_1(x,y)U_1^*(x,y) + \\ &U_0 U_1^*(x,y)e^{i\alpha x} + U_0^* U_1(x,y)e^{-i\alpha x}\end{aligned}\tag{2}$$

where $\Im$ indicates the Fourier transform operator, and $\tilde{I}$ is the Fourier transform of I. Using the correlation theorem and the fact that U_0 is uniform after spatial filtering, Eq. (2) becomes

$$\begin{aligned}\tilde{I}(k_x,k_y) = |U_0|^2\,\delta(k_x,k_y) + &\tilde{U}_1(k_x,k_y)\otimes\tilde{U}_1(k_x,k_y) \\ &U_0\tilde{U}_1(-k_x-\alpha,-k_y) + U_0\tilde{U}_1(k_x+\alpha,k_y)\end{aligned}\tag{3}$$

where $\otimes$ indicates the convolution operation. Equation (3) provides insights into the frequency coverage of the interferogram, as follows. Since U_1 is diffraction limited, it is a band-limited signal, with its maximum frequency governed by the NA of the objective, $k_{max} = \beta$NA, $\beta = \omega/c$. Since the correlation term, $\tilde{U}_1 \otimes \tilde{U}_1$ has a maximum frequency of 2βNA, we find that the minimum modulation frequency must be $\alpha \geq 3\beta$NA. On the other hand, the maximum frequency of the entire signal is 4βNA. According to the Nyquist theorem, the pixel sampling frequency, k_p, must satisfy $k_p \geq 8\beta$NA.

In PSwDPM, the correlation term is subtracted out, such that α can be lower, namely, $\alpha = \beta$NA, without loss of information. As a result, the highest frequency of the signal is $k_{max}' = 2\beta$NA, and the new pixel sampling frequency is $k_p' \geq 4\beta$NA. Thus, the space-bandwidth product is twice longer. An illustration of these sampling conditions can be found in Fig. 2 of Ref [26]. Note that, in on-axis methods, the auto correlation term is eliminated via phase shifting and $\alpha = 0$. In this case, the highest frequency is simply $k_{max}'' = \beta$NA, and the pixel sampling condition is $k_p'' \geq 2\beta$NA. Thus, it is apparent that by collecting two phase shifted frames, one gains a factor of 2 in space-bandwidth product, while collecting 4 improves the product by a factor of 4.

Figure 2(a) shows an example of the measured interferogram. Usually, this image is Fourier transformed, which results in a spatial power spectrum as illustrated in Fig. 2(c). The DC and one of the orders are filtered out and the resulting signal Fourier transformed back to the spatial domain. This procedure amounts to a Hilbert transform and yields the complex analytic signal associated with $\cos[\phi(x,y) + \alpha x]$, the argument of which gives the phase of interest, ϕ. We show that by shifting the grating by half its period, i.e., by $x_0 = \pi/\alpha$, and recording the two respective interferograms, we can eliminate the autocorrelation, i.e., the DC term in Fig. 2(c), thus, extending the frequency coverage of the first order. This result is illustrated in Fig. 2(d). For this proof of principle study, we shifted the grating manually using a precision translation stage. In essence, by acquiring two different interferograms and subtracting them, $I(0) - I(\pi) = 4\sqrt{I_0 I_1}\cos\left[\varnothing(x,y) + ax\right]$, we obtain a phase image of higher resolution, as seen by comparing Fig. 2(f) *vs.* 2e.

Optics EXPRESS

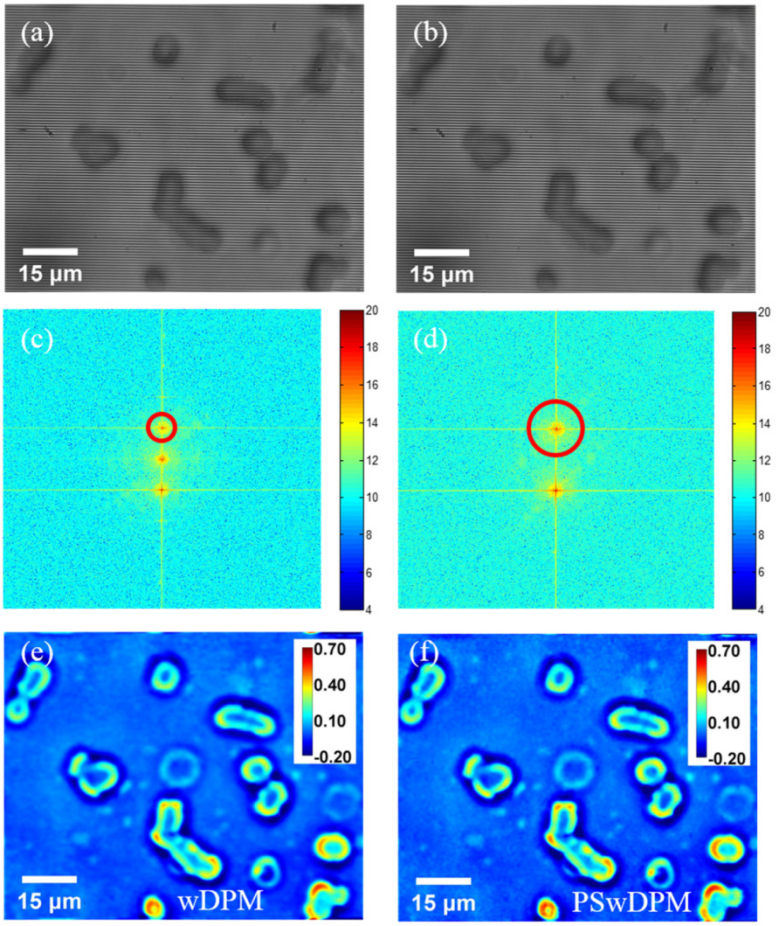

Fig. 2. wDPM vs. PSwDPM applied to image a blood smear. (a) Interferogram $I(0)$; (b) Interferogram $I(\pi)$; (c) Power spectrum of $I(0)$; (d) Power spectrum of $I(0)$-$I(\pi)$; Reconstructed phase obtained by wDPM (e) and PSwDPM(f). Colorbars in c-d indicate intensity in log scale and arbitrary units and in e-f show phase in rad, as indicated.

3. Results

In order to demonstrate the resolution gain of PSwDPM, we imaged both test samples and biological samples. Figure 3 shows the comparison between the performance of regular wDPM and PSwDPM when imaging an Airforce target. We perform the side by side comparison as a function of the digital filter (F) applied in the in the spectral domain. Thus, F = 1.0 corresponds to the diameter of the circle in Fig. 2(d) that touches the zero-frequency point. This is the maximum frequency coverage that can be retrieved from the sample and is only available when the DC is eliminated via phase shifting. When the DC order is present, F = 1 results in strong overlap between the frequencies of the first and zeroth order, i.e., *aliasing*. Note that for all values of F, the spatial phase noise is lower for the phase shifting method (Figs. 3(a)-3(h)). These results indicate also that for $F \geq 0.5$, the wDPM suffers from aliasing, which becomes severe for F = 1.0. PSwDPM is free of these artifacts for all F-values. Figure 3(i) shows the high frequency boost in PSwDPM compared to the artifact-free wDPM (F = 0.3).

Optics EXPRESS

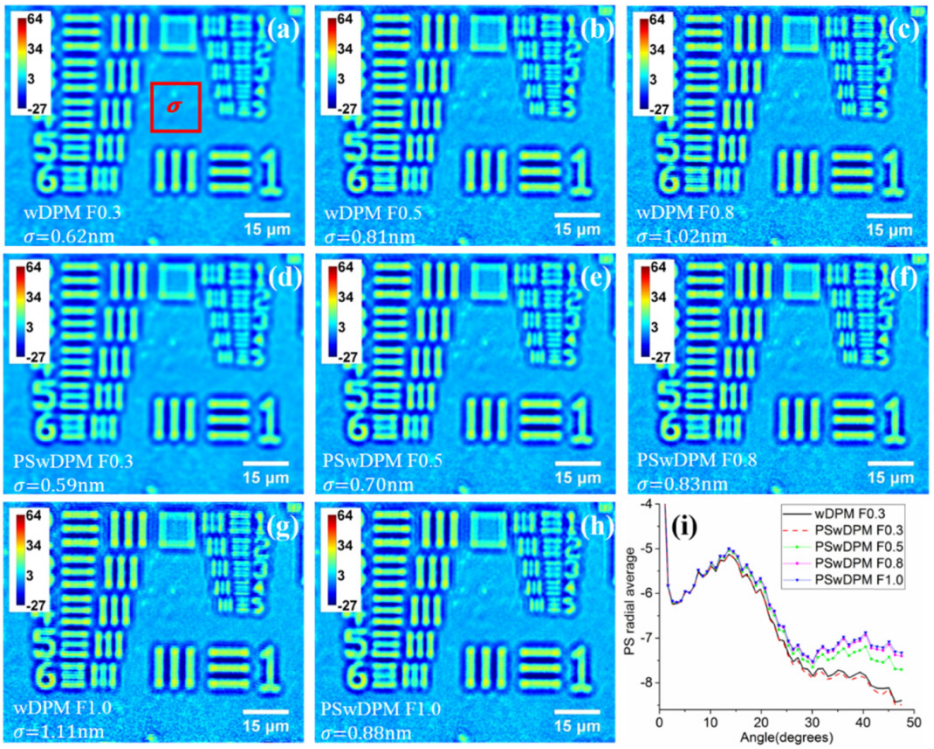

Fig. 3. (a-h) Height maps of USAF resolution target with different BPF size, with the color bar indicates height in nm. (i) Angular spectrum

Next, we illustrate the increased performance by imaging an unlabeled prostate tissue biopsy. Figures 4 show the comparison between regular wDPM and PSwDPM imaging. Again, the aliasing artifact due to the frequency overlap in the spectrum domain is apparent for wDPM, at $F \geq 0.5$.

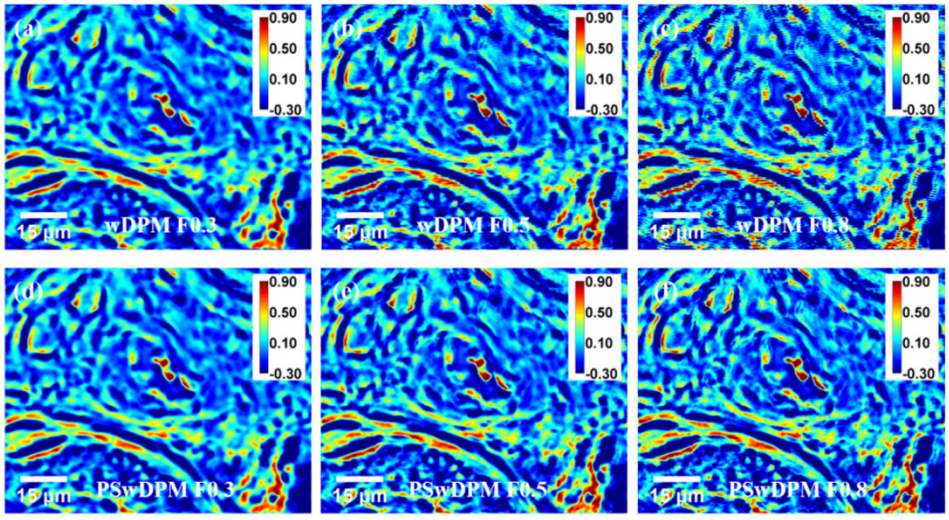

Fig. 4. Phase maps of an unlabeled prostate biopsy obtained by wDPM and PSwDPM, with the color bar indicating phase in radians.

Optics EXPRESS

4. Summary and discussion

In summary, we developed PSwDPM to combine phase-shifting and off-axis techniques and overcome the original space-bandwidth product of the image. Of course, we achieve this at the expense of acquisition rate. In contrast to wDPM, PSwDPM is no longer single shot and instead requires the acquisition of two subsequent interferograms. Note that the acquisition rate of PSwDPM is still faster than phase shifting methods, which typically require four frames. Thus, we expect that our new technique will be most practical in applications that require the largest resolution and field of view possible.

Acknowledgements

This work was supported by the National Science Foundation (CBET-0939511 STC, DBI 14-50962 EAGER, IIP-1353368). For more information, visit http://light.ece.illinois.edu/. Mingguang Shan was supported by National Natural Science Foundation of China (61377009), Major National Scientific Instrument and Equipment Development Project of China (2013YQ290489), China Scholarship Council (201506685053), Heilongjiang Science Foundation of China (F201411), and Fundamental Research Funds for the Central Universities of China.